

Measuring Marine Infrared Clutter

Kim T. Constantikes and Emily D. Claussen

During field tests, researchers measure marine clutter with an infrared camera. These data are being used to study infrared seeker performance, test image processing algorithms, and validate Seascope, an ocean clutter synthesis model. Thus far, data have been collected from the West River of the Chesapeake Bay and offshore from Atlantic City, New Jersey. A future study is planned at a site having fewer offshore shoals and more long-scale gravity wave content.

INTRODUCTION

The Applied Physics Laboratory's Electro-Optical Systems Group is conducting infrared measurements of the marine environment for infrared seeker performance analysis, image processing algorithm development, statistical clutter characterization, and validation of our marine clutter model, Seascope. We have collected radiometrically calibrated back- and side-lighted cloud clutter, solar ocean glint, and skylit ocean clutter data in the midwave and have calculated spatially local estimates of image radiance mean, variance, and correlation time.

METHOD

Our measurement apparatus consists of a liquid-nitrogen-cooled indium antimonide focal plane array camera (Cincinnati Electronics IRC160), two Hi-8mm visible band camcorders, and a sighting telescope, all mounted on a common tripod head. Two workstations collect and analyze the data. Additional instruments collect environmental parameters and determine geolocation. We have made the apparatus compact and efficient to minimize field test expense and logistic complications.

The infrared camera uses a 25-, 50-, or 100-mm telescope with a resolution of 2.0, 1.0, or 0.5 mrad, respectively, to produce an image of 120 rows by 160

columns of pixels. An adjustable aperture can be added to restrict the entrance aperture of the optics and thus reduce the radiant flux reaching the focal plane. The camera noise effective ΔT is 40 mK at 300 K. A cold filter installed on the focal plane Dewar controls the spectral passband of the camera, currently 2.3 to 4.6 μm . Other filters can be used.

We radiometrically calibrate using extended-area blackbody sources that bracket the measurement radiance range. Images are captured at a rate up to 51 Hz with integration times from 0.3 to 19.0 ms. Detector outputs are digitized to a resolution of 12 bits, an instantaneous dynamic range of 72 dB. Downloadable tables within the camera compensate for nonuniform diode response. Compensation is infrequently required because the indium antimonide diodes have good long-term stability. A parallel data bus transmits digitized data to a 4-megabyte shared memory installed in a PC. Video in black and white or pseudocolor is also output from the camera head. This video output is recorded by one of the camcorders mounted on the tripod head. The camcorder viewfinder serves as a color viewfinder for the infrared camera, providing good visibility in high-ambient-light conditions.

Up to 109 frames of the digital output of the infrared camera are captured at the frame rate (51 Hz) or integer-divided rates down to 5.1 Hz. The clutter scenes

can be sampled with a temporal resolution of 20 ms for 2.1 s up to a resolution of 200 ms for 21 s. Data collection is under control of programs that additionally provide for calibration, basic statistical analysis, and nonuniformity compensation. These programs also append tripod angles, time, and other site- and measurement-specific information to the image file. Much of this information is manually entered at the time, but we have plans to automate collection of these data as well.

The second Hi-8mm camcorder visibly records each measurement. We start the camcorders a few seconds before digital infrared data collection is begun and stop a few seconds after data collection is completed. The video record is kept as short as possible for ease of reviewing after the field measurement. Both camcorders have time annotated on the recording, and digital files are named using time so that video is easily associated with the digital data. The audio recording of one camcorder provides voice annotation. Eventually, the two camcorders will be controlled by the data collection PC.

A second computer provides on-site data analysis and data storage capability. We use either a Silicon Graphics Indigo or a Pentium-based PC running a UNIX operating system. Data are stored on digital audio tape having about 2 gigabytes of capacity per tape. One tape is sufficient for a day of operation. We use the Khoros data visualization package to quickly construct data analysis operations described graphically as signal flow graphs. We routinely check histograms, descriptive statistics, image animations, and radiometric calibrations. A thin-wire Ethernet local area network is used to interface the data collection computer and data analysis computer. Data on the data collection computer are exported to the analysis computer using Network File System Protocol. Thus, data may be analyzed concurrently with data collection. Serial Line Internet Protocol and a high-speed telephone modem connect the data collection computer to the outside world. We use the Mosaic World Wide Web browser to access weather predictions and satellite imagery available on the Internet to plan activities. Selected data are transmitted to computers at APL for in-depth analysis while the measurement team is in the field.

Tripod location and true north are determined by a handheld Garmin Global Positioning System. Temperature and humidity probes are used to collect basic environmental data. Either World Wide Web weather data or National Weather Service weather radio transmissions are used for additional data such as offshore buoy wind speed and direction.

The measurement apparatus described is compact and portable. All the instruments and support equipment fit into a small van, and only two operators are needed.

Thus, the field test is conducted at minimal expense while allowing for data analysis at the field site. We are constructing a second version of this apparatus in which almost all functions will be automated, and only one laptop computer will be required instead of the two workstations we currently use. All the equipment, excluding liquid nitrogen, can be contained in three cases for ease of portability to any field test site. Other infrared cameras can be added to the tripod head in order to measure different spectral bands simultaneously.

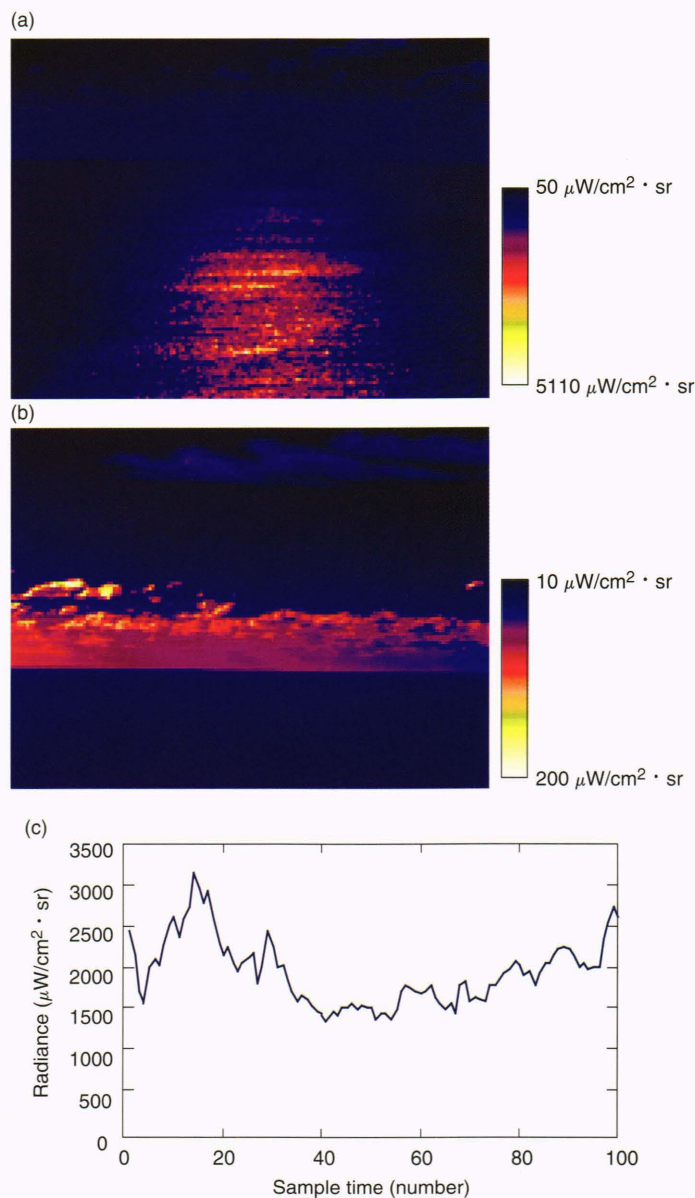


Figure 1. Sample data from our Atlantic City measurement. (a) The solar glint corridor at about 7:55 a.m. (b) Side- and back-lighted clouds on the horizon at about 8:20 a.m. The images in parts a and b are taken from a 20-s time series. The color bars on the right indicate the radiance scale associated with each image. (c) The radiance of a single pixel (80, 78) from the glint corridor of the image in part a as a function of sample time (number).

RESULTS

We have used our apparatus for two data collections to date. The first test, in November 1994, was a measurement from a pier in the West River of the Chesapeake Bay. Sun glinting from the bay was measured from a 2-m altitude and up to 20° declinations, yielding centimeter spatial and 20-ms temporal resolution data. These are being used to validate the ability of our ocean clutter synthesis model to reproduce sun glint scintillation and thereby the small-scale water wave and light transport models we use. Our second exercise, in December 1994, was a measurement taken from about a 100-m altitude looking offshore from Atlantic City, New Jersey. We measured back- and side-lighted cloud clutter, solar ocean glint, and skylit ocean clutter with spatial resolutions of 0.5, 1.0, and 2.0 mrad and with temporal resolutions of 20 and 200 ms. Figure 1 shows some selected images. These data will be used to test image processing algorithms¹ and for validation of the large-scale water wave and light transport models in our clutter synthesis.

Results of our preliminary statistical characterization are shown in Figure 2. Note the spatially periodic variation of the mean glint intensity from near field toward the horizon (Fig. 2b). We hypothesize that this variation is due to shoal formation in shallow water, whereby the shoals reduce the effective albedo of the surface via wave modification. Also note that diagonal streaks are present in the row and column versus time presentations of glint (Fig. 2a). It may be possible, in principle, to distinguish glint from other moving objects using spatiotemporal matched filters if enough is known about the image and clutter geometry and sufficient look time is available. In the near field, the correlation time of the glint corridor is shorter than in the surrounding water (Fig. 2d). We hypothesize that this result is due to millimeter-sized specularly reflecting facets that propagate rapidly in comparison with the larger scale gravity waves that produce the variation in radiance away from the specular point by diffuse reflection of sky radiance. The difference in correlation time should be more pronounced with a smaller instantaneous (detection) field of view. In these figures, the footprint, or integrating area, of a single detector is about 0.25 m^2 in the near field. The spatial averaging will tend to increase the correlation time estimates. Also, the correlation time associated with the horizon is very short, indicating that the dominant random process is sensor noise, which is uncorrelated. Cloud edges have shorter correlation times because significant motion of the clouds occurred during one data collection sequence.

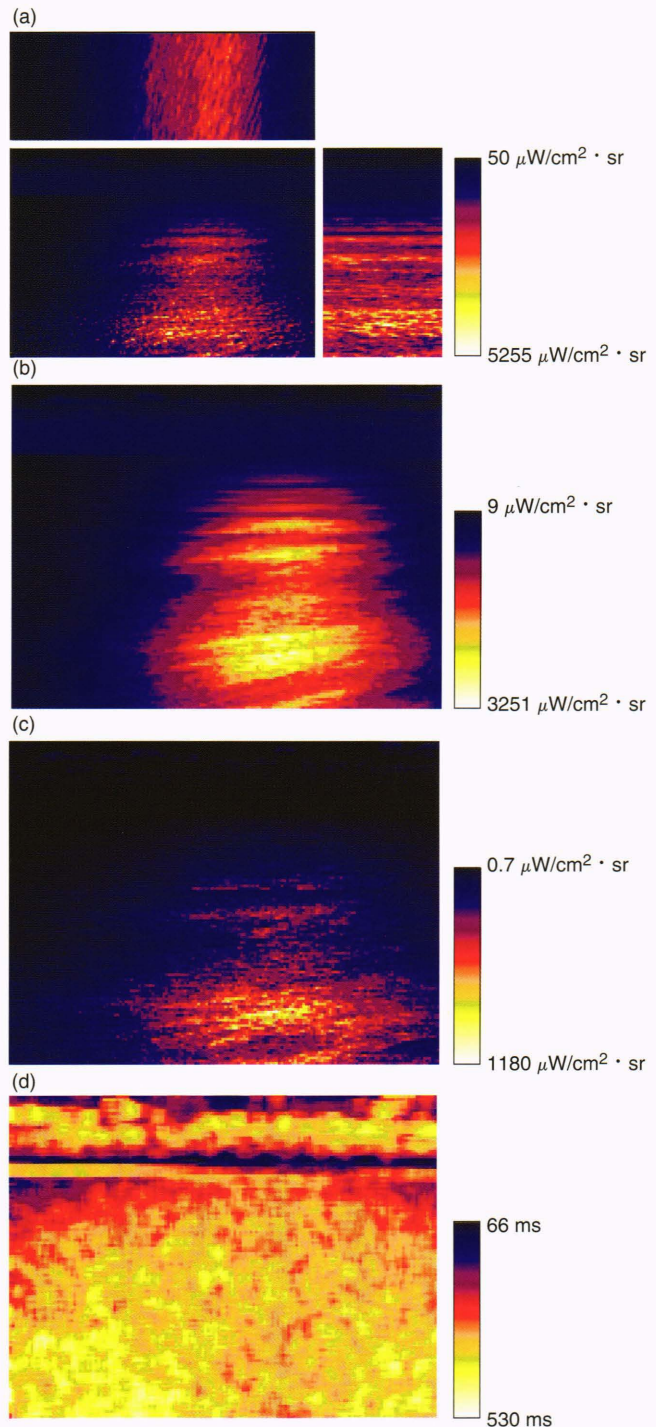


Figure 2. Visualization and statistics of glint clutter. (a) A “cube” of data, i.e., the spatial and temporal image, showing a row and column of data in time. This image was taken at a rate of 5 Hz and shows spatiotemporal correlations. (b) and (c) The spatial distribution of the image temporal mean and standard deviation, respectively. The color bars on the right of parts a, b, and c indicate the radiance scale associated with each image. (d) A portrayal of the spatial distribution of correlation time in an image taken at a rate of 51 Hz. The corresponding color bar shows the relationship between color and α -dependent correlation time, which is the correlation time of an assumed exponentially correlated process. Correlation time was determined by sample periodogram estimates over a 64-frame time series and averaged over 5×5 pixel spatial neighborhoods.

FUTURE WORK

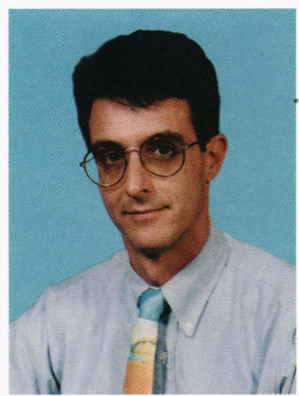
Our next measurement is planned at a location with fewer offshore shoals and more long-scale gravity wave content. We will use two midwave cameras and one longwave camera in this experiment, intended to confirm our ability to predict radiance in one midwave band from the measurement of radiance in a disjoint band. Long-wave data will be collected to determine

if glint clutter temporal and spatial statistics are the same as in the midwave, and all three bands will be used to validate our treatment of infrared surface phenomenology and radiative transport in Seascape.

REFERENCES

¹Constantikes, K. T., "Point Detection Using a Coning Scan Imager," *Johns Hopkins APL Tech. Dig.* 15(3), 242-249 (1994).

THE AUTHORS



KIM T. CONSTANTIKES is a Senior Staff engineer in APL's Fleet Systems Department. He received his B.S. degree in applied physics in 1983 from Ohio University. He then attended Carnegie Mellon University with a Benjamin Franklin Fellowship and received an M.S. degree in electrical and computer engineering in 1985. At Carnegie Mellon, he researched topics in pattern recognition and sensors in the Smart Sensors Laboratory of the Robotics Institute. Mr. Constantikes joined APL's Electro-Optical Systems Group in 1985, where he has worked on various computational and algorithmic aspects of imaging systems used for target acquisition, tracking, and recognition, as well as image-matching navigation. His current interests include image and scene modeling, image processing algorithms, target detection in clutter, and computer graphics. His e-mail address is Kim.Constantikes@jhuapl.edu.



EMILY D. CLAUSSEN received a B.S. degree in electrical engineering from Purdue University in 1994. She has been an Associate Staff engineer in APL's Electro-Optical Systems Group since joining APL in June 1994. Currently working on midwave measurements of marine environments, she has also contributed to the analysis of image processing algorithms for an infrared seeker. She is an active member of the Baltimore-Washington Section of the Society of Women Engineers. Her e-mail address is Emily.Claussen@jhuapl.edu..